Physica A 410 (2014) 88–93

Contents lists available at ScienceDirect

Physica A

journal homepage: www.elsevier.com/locate/physa

Detection of anyon's braiding and identification of anyon entangled states in optical microcavities

Yao Shen [a,b,c], Qing Ai [d], Gui Lu Long [a,b,c,*]

[a] State Key Laboratory of Low-Dimensional Physics and Department of Physics, Tsinghua University, Beijing 100084, China
[b] Collaborative Innovation Center of Quantum Matter, Beijing 100084, China
[c] Tsinghua National Laboratory For Information Science and Technology, Beijing 100084, China
[d] Department of Chemistry, National Taiwan University, Taipei City 106, Taiwan

HIGHLIGHTS

- Simulate anyon in a composite system of microcavities and quantum dots.
- Dynamically detect braiding operations of anyon for a minimum unit of four qubits.
- Discriminate anyon entangled states based on the above method.

ARTICLE INFO

Article history:
Received 4 January 2014
Received in revised form 9 March 2014
Available online 13 May 2014

Keywords:
Anyons
Braiding detecting gate
Bell states

ABSTRACT

In this paper, a simulation of anyon states in a composite system of quantum dots and optical microcavities is introduced. We construct a novel quantum gate, the braiding detecting gate (BDG), by making use of interactions between the quantum-dot electron spins in optical microcavities and photons to detect the dynamic braiding operation of anyons. Additionally, by means of the BDGs, we also present a protocol to distinguish different entangled states of anyons.

1. Introduction

In the experimental investigations of the fractional quantum Hall effect [1,2], a kind of quasiparticle in two dimensions is discovered, namely anyon. This kind of quasiparticle is famous for its amazing properties [1,3–5]. Anyons obey fractional statistics, which is characterized by a fractional statistical parameter and belongs to intermediate statistics [6]. Therefore, studies on anyons have become an important branch of modern physics [7–27]. Generally, anyons of each type cannot be created singly but in pairs. When two different kinds of anyons braid, there will be an additional phase factor added to the wave function of the system. In recent years, based on these discoveries, several theoretical models of anyons were put forward. One of the exactly solvable models is the first Kitaev model [28,29], which has been experimentally realized in photonic [20] and NMR [27] systems. The original model is a honeycomb lattice model with spin-1/2 system. Through the perturbation theory, the model can be changed into a quadrangular lattice model with a spin on each edge of the quadrangle. The vacuum, e particle, m particle and $\varepsilon = e \times m$ are four superselection sectors of the first Kitaev model. When we use

* Corresponding author at: State Key Laboratory of Low-Dimensional Physics and Department of Physics, Tsinghua University, Beijing 100084, China. Tel.: +86 10 62772692; fax: +86 10 62772692.
E-mail addresses: gllong@tsinghua.edu.cn, gllong@mail.tsinghua.edu.cn (G.L. Long).

http://dx.doi.org/10.1016/j.physa.2014.05.022
0378-4371/

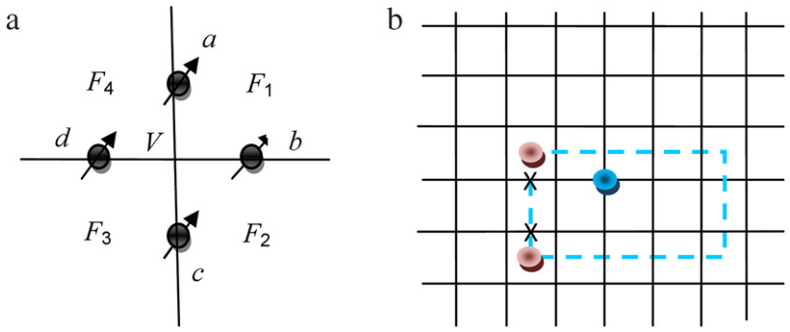

Fig. 1. (a) The minimum unit for anyon statistics. In the first Kitaev model, a, b, c, d are four spins. V is a vertex and F_1, F_2, F_3, F_4 are four faces. e and m particles are generated on the vertices and faces, respectively. (b) The braiding operation of anyons in the first Kitaev model is to move particles by means of applying Pauli operations on the spins in turn.

a Pauli Z operator on a spin laid on the edge, two e particles are created on the two vertices of that edge. When a Pauli X operation is applied on a spin, two m particles are generated on the two faces connected to the edge.

As a spin-1/2 system, electron spins are a natural candidate for realizing such anyon systems. A charged quantum dot in optical microcavities can create particles with negative charges. These particles are electrons restricted in one hole. When a photon interacts with these electrons, the whole system acts like a beam splitter in the limit of weak fields [30]. Since the photon–electron interaction will change the photon's state in a given way while unperturbing the spin's state, we can simulate the first Kitaev model and construct the braiding detecting gate (BDG) to detect the braiding operation in the composite system of four quantum dots and optical microcavities. Applying the BDG, we can dynamically monitor the process of braiding meanwhile undisturbing the system.

On the other hand, as known to all, quantum entanglement plays an important role in the quantum information processing. For example, it accelerates the computation of quantum computers [31–35], dense coding [36,37], quantum-state sharing [38–40] and quantum key distribution [41–45]. Entanglement purification [46–52] and concentration [53–58] are two kinds of ways to distill subsets of maximal entangled states. Because anyons are created in pairs, the quantum entanglement states of anyons are very common in reality. Therefore, it becomes urgent to distinguish different entanglement states of anyons in the quantum information processing of anyons. In this paper, we also put forward a method to distinguish different anyon entangled states utilizing the BDG realized in the above quantum-dot and optical-microcavity systems.

This paper is organized as follows. In Section 2, the anyon state is simulated in the composite system of quantum dots and optical microcavities and the BDG is constructed to observe the braiding operation. In Section 3, we propose a protocol to identify different types of anyons and their entangled states. Finally, the main points are summarized in the Conclusion part.

2. The braiding detecting gate

Recently, Xi and Hu proposed a new method to demonstrate anyon statistics [59], where only four qubits are required to create anyons and demonstrate the braiding operation (see Fig. 1(a)). The Hamiltonian of our system is

$$H = -A_v - B_{F_1} - B_{F_2} - B_{F_3} - B_{F_4}, \tag{1}$$

where $A_v = X_a X_b X_c X_d$, $B_{F_1} = Z_a Z_b$, $B_{F_2} = Z_b Z_c$, $B_{F_3} = Z_c Z_d$, and $B_{F_4} = Z_a Z_d$. The braiding operation where one anyon moves around another is one of the most distinct properties of anyons. When different kinds of anyons braid with each other, an additional phase factor appears in the wavefunction of the system. In the case of the first Kitaev model, the phase factor is -1. For example, when an m particle goes around an e particle for one circle, there will be a π phase in addition to the original wavefunction. On the other hand, when these two particles are of the same kind, e.g., two m particles or two e particles, the wavefunction remains itself after braiding. To realize the braiding operation in the first Kitaev model, Pauli X and Pauli Z operators are needed, cf. Fig. 1(b). e particles are created in pairs on the vertices of the quadrangle using the Pauli Z operator. Moving the e particle means applying Z operators on the spins sequentially. m particles are generated in pairs on the faces of the quadrangle through the Pauli X operator. Moving the m particle means applying X operators on the spins in turn.

In the first Kitaev model, by defining the single electron spin states $|\uparrow\rangle \equiv |0\rangle$ and $|\downarrow\rangle \equiv |1\rangle$, the braiding operation can be constructed as follows:

$$Z_a X_a X_d X_c X_b Z_a, \tag{2}$$

where $Z_a(X_a)$ is the Pauli $Z(X)$ gate on spin a (see Fig. 1). The BDG can show us dynamically the braiding operation between e particle and m particle.

We propose realizing the qubits by means of the quantum-dot electron spins in microcavities with $|\uparrow\rangle$ and $|\downarrow\rangle$ denoting the polarized spin states. When a photon passes through a microcavity, it interacts with the electrons. Inside the microcavity,

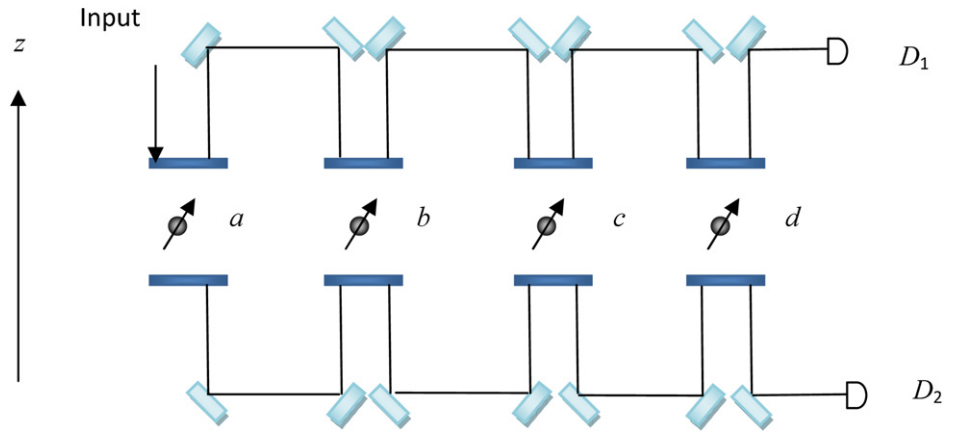

Fig. 2. Schematic diagram of the BDG. This quantum gate consists of four quantum dot electron spins a, b, c, d in the optical microcavities. D_1 and D_2 are two single-photon detectors. A left-circular-polarized photon which propagates against the z axis is input from the left of the system.

Table 1
Relevant eigen states and quasiparticles used in the present scheme. The corresponding outgoing photon states after interacting with the four spins sequentially are listed in the third column.

Eigen vector	Quasiparticle	Response
$(\|1110\rangle - \|0001\rangle)/\sqrt{2}$	2m+e	$\|R^{\downarrow}\rangle$
$(\|1101\rangle - \|0010\rangle)/\sqrt{2}$	2m+e	$\|R^{\downarrow}\rangle$
$(\|1011\rangle - \|0100\rangle)/\sqrt{2}$	2m+e	$\|R^{\downarrow}\rangle$
$(\|0111\rangle - \|1000\rangle)/\sqrt{2}$	2m+e	$\|R^{\downarrow}\rangle$
$(\|1001\rangle - \|0110\rangle)/\sqrt{2}$	2m+e	$\|L^{\uparrow}\rangle$
$(\|1100\rangle - \|0011\rangle)/\sqrt{2}$	2m+e	$\|L^{\uparrow}\rangle$
$(\|0001\rangle + \|1110\rangle)/\sqrt{2}$	2m	$\|R^{\downarrow}\rangle$
$\|e\rangle \equiv (\|1111\rangle - \|0000\rangle)/\sqrt{2}$	e	$\|L^{\uparrow}\rangle$
$\|v\rangle \equiv (\|0000\rangle + \|1111\rangle)/\sqrt{2}$	vacuum	$\|L^{\uparrow}\rangle$

$|R^{\uparrow(\downarrow)}\rangle(|L^{\uparrow(\downarrow)}\rangle)$ represents right(left)-circular-polarized photon states and the superscript arrow $\uparrow$ $(\downarrow)$ describes the propagation direction of the photon along(against) the z axis. For example, $|R^{\uparrow}\rangle$ means that a photon with right-circular-polarized propagates along the z axis. The photon–electron interaction is usually described as [30]

$$\begin{aligned}
&|R^{\uparrow},\uparrow\rangle \to |L^{\downarrow},\uparrow\rangle, \qquad |R^{\uparrow},\downarrow\rangle \to -|R^{\uparrow},\downarrow\rangle,\\
&|R^{\downarrow},\downarrow\rangle \to |L^{\uparrow},\downarrow\rangle, \qquad |R^{\downarrow},\uparrow\rangle \to -|R^{\downarrow},\uparrow\rangle,\\
&|L^{\uparrow},\downarrow\rangle \to |R^{\downarrow},\downarrow\rangle, \qquad |L^{\uparrow},\uparrow\rangle \to -|L^{\uparrow},\uparrow\rangle,\\
&|L^{\downarrow},\uparrow\rangle \to |R^{\uparrow},\uparrow\rangle, \qquad |L^{\downarrow},\downarrow\rangle \to -|L^{\downarrow},\downarrow\rangle.
\end{aligned} \tag{3}$$

Since in the anyon statistics the minimum unit is four, we consider four spins in optical microcavities. These four spins are labeled as a, b, c, d as shown in Fig. 2. For a photon interacting with four spins, there are 16 possible cases on account of all possible spin states. Without loss of generality, we consider a left-circular-polarized photon which propagates against the z axis, i.e., $|L^{\downarrow}\rangle$. Having interacted with the four spins sequentially, the outgoing photons are detected by the two detectors on the right. By using Eq. (3), we can directly write the interaction as

$$|L^{\downarrow},M\rangle \to \begin{cases} |L^{\uparrow},M\rangle, & \text{for } \langle M|\sum_j s_j^z|M\rangle = \text{even},\\ -|R^{\downarrow},M\rangle, & \text{for } \langle M|\sum_j s_j^z|M\rangle = \text{odd}, \end{cases} \tag{4}$$

where the four spin states are $|M\rangle = |0000\rangle, |0001\rangle, \ldots, |1111\rangle$, and s_j^z is the jth spin operator in the z direction. In other words, when there are even number of spins polarized in the z direction, a left-circular-polarized photon will transmit in the z direction and thus is detected by the detector D_1. Otherwise, the other detector D_2 will respond. Since for two states with the same parity the outgoing photons are of the same properties, it can be straightforwardly shown that when the system is in the eigen states of the first Kitaev model with four qubits, the two detectors will give the definite response while the system is left unchanged. The nine relevant eigen states of the four-qubit Kitaev model and their corresponding responses are explicitly depicted in Table 1.

Table 2
Each operation and its resulted state for our scheme. The detected photon states are shown in the right column.

Operation and state	Response
$\|v\rangle = (\|0000\rangle + \|1111\rangle)/\sqrt{2}$	$\|L^{\uparrow}\rangle$
$\|\psi_1\rangle = Z_a\|v\rangle = (\|1111\rangle - \|0000\rangle)/\sqrt{2}$	$\|L^{\uparrow}\rangle$
$\|\psi_2\rangle = X_b\|\psi_1\rangle = (\|1011\rangle - \|0100\rangle)/\sqrt{2}$	$\|R^{\downarrow}\rangle$
$\|\psi_3\rangle = X_c\|\psi_2\rangle = (\|1001\rangle - \|0110\rangle)/\sqrt{2}$	$\|L^{\uparrow}\rangle$
$\|\psi_4\rangle = X_d\|\psi_3\rangle = (\|1000\rangle - \|0111\rangle)/\sqrt{2}$	$\|R^{\downarrow}\rangle$
$\|\psi_5\rangle = X_a\|\psi_4\rangle = (\|0000\rangle - \|1111\rangle)/\sqrt{2}$	$\|L^{\uparrow}\rangle$
$\|\psi_6\rangle = Z_a\|\psi_5\rangle = -\|v\rangle$	$\|L^{\uparrow}\rangle$

Table 3
Each operation and its resulted state for the scheme in Ref. [59]. The detected photon states are shown in the right column.

Operation and state	Response
$\|v\rangle = (\|0000\rangle + \|1111\rangle)/\sqrt{2}$	$\|L^{\uparrow}\rangle$
$\|\psi_1\rangle = \sqrt{Z_a}\|v\rangle = (i\|0000\rangle - \|1111\rangle)/\sqrt{2}$	$\|L^{\uparrow}\rangle$
$\|\psi_2\rangle = X_c\|\psi_1\rangle = (i\|0010\rangle - \|1101\rangle)/\sqrt{2}$	$\|R^{\downarrow}\rangle$
$\|\psi_3\rangle = X_d\|\psi_2\rangle = (i\|0011\rangle - \|1100\rangle)/\sqrt{2}$	$\|L^{\uparrow}\rangle$
$\|\psi_4\rangle = X_a\|\psi_3\rangle = (i\|1011\rangle - \|0100\rangle)/\sqrt{2}$	$\|R^{\downarrow}\rangle$
$\|\psi_5\rangle = X_b\|\psi_4\rangle = (i\|1111\rangle - \|0000\rangle)/\sqrt{2}$	$\|L^{\uparrow}\rangle$
$\|\psi_6\rangle = X_c\|\psi_5\rangle = (i\|1101\rangle - \|0010\rangle)/\sqrt{2}$	$\|R^{\downarrow}\rangle$
$\|\psi_7\rangle = \sqrt{Z_a}\|\psi_6\rangle = -i(\|1101\rangle + \|0010\rangle)/\sqrt{2}$	$\|R^{\downarrow}\rangle$
$\|\psi_8\rangle = X_c\|\psi_7\rangle = -i\|v\rangle$	$\|L^{\uparrow}\rangle$

In our scheme, cf. Table 2, after preparing the system in the ground state, cf. Ref. [59], we firstly apply a Z_a operation to create an e particle in the vertex. And then it is followed by four X operations on the four qubits in turn. Finally, another Z_a operation is applied to annihilate the e particle and the vacuum is recovered. During these processes, after every operation, a left-circular-polarized photon is sent to detect the state of the system. Because in each state the system has a definite parity, the system remains in the same state as that before detection. Therefore, the BDG can non-destructively detect the state while the braiding operation can resume after detection.

Furthermore, in the previous schemes, cf. Refs. [21,20,59], a Ramsey-type interference experiment proposal was utilized to observe the additional phase as a result of the braiding operation. In order to realize the proposal, the system was initially prepared in the superposition of $|v\rangle$ and $|e\rangle$ by a $\sqrt{Z_a}$ operation with

$$\sqrt{Z} = \begin{pmatrix} i & 0 \\ 0 & -1 \end{pmatrix} \tag{5}$$

in the $\{|0\rangle, |1\rangle\}$ basis, or equivalently

$$\sqrt{Z} = \frac{1}{2}\begin{pmatrix} i-1 & -(i+1) \\ -(i+1) & i-1 \end{pmatrix} \tag{6}$$

in the $\{|v\rangle, |e\rangle\}$ basis. Our gate also works in their proposal, as shown in Table 3. Although their scheme begins from a superposition of quasi-particle eigen states, the state after every manipulation also has a definite parity. In this case, by monitoring the response of the two detectors, we can dynamically observe the braiding operation in addition to the additional phase at the end.

3. The identification of anyons and their entangled states

Entanglement is a valuable resource in quantum information processing. In this section, we give a protocol to distinguish different entangled states of anyons. To be specific, we discuss two-anyon entangled states, i.e. Bell states.

As shown in Fig. 3, there are two parts, i.e., A and B, making up this system. They are far from each other but entangled with each other. Parts A and B are both the minimum units for anyons as depicted in Fig. 2. As stated above, there are two kinds of anyons, e particles and m particles. We assume that there already exists an e particle on the vertex V or two m particles on the faces F_3 and F_4 (see Fig. 1) of each part. Here the eigen vectors of the space are assumed to be $\{|e_Ae_B\rangle, |e_Am_B\rangle, |m_Ae_B\rangle, |m_Am_B\rangle\}$, where we define $|m\rangle \equiv (|0001\rangle + |1110\rangle)/\sqrt{2}$. In this case, four Bell states of this A–B system become

$$|\Phi_{AB}^{\pm}\rangle = \frac{1}{\sqrt{2}}(|e_Ae_B\rangle \pm |m_Am_B\rangle), \tag{7}$$

$$|\Psi_{AB}^{\pm}\rangle = \frac{1}{\sqrt{2}}(|e_Am_B\rangle \pm |m_Ae_B\rangle). \tag{8}$$

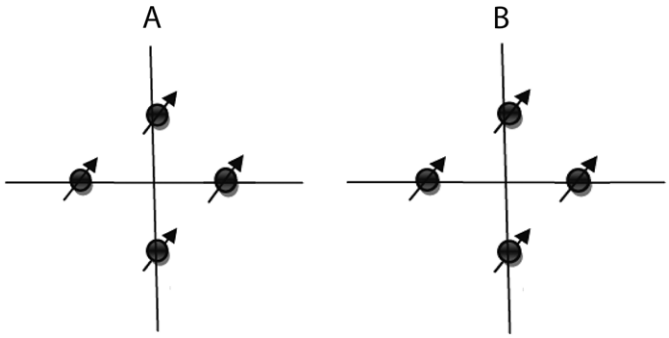

Fig. 3. Identification of two-anyon entangled states. Two entangled parts A and B constitute the system. Each part has four spins in optical microcavities as detailed in Fig. 2.

To identify these four Bell states, we only need two steps. First of all, two left-circular-polarized photons which propagate against the z axis are respectively sent to the two subsystems. Since $|e\rangle$ and $|m\rangle$ have different parities, if the system is initially in the states $|\Phi_{AB}^{\pm}\rangle$, both the same detectors $D_1(D_2)$ will respond and thus the spins are projected to the product state $|e_Ae_B\rangle(|m_Am_B\rangle)$. Otherwise, if the system is initially in the states $|\Psi_{AB}^{\pm}\rangle$, two different detectors will respond and thus the spins are projected to the product state $|e_Am_B\rangle$ or $|m_Ae_B\rangle$. In this way, $|\Phi_{AB}^{\pm}\rangle$ are discriminated from $|\Psi_{AB}^{\pm}\rangle$.

In the second step, we perform a unitary transformation U on both subsystems with

$$U \equiv \frac{1}{\sqrt{2}}\begin{pmatrix} 1 & -1 \\ 1 & 1 \end{pmatrix} = \sqrt{Z_a} \otimes \sqrt{X_d} \tag{9}$$

in the basis of $\{|e\rangle, |m\rangle\}$. It simply rotates $|e\rangle$ to $(|e\rangle + |m\rangle)/\sqrt{2}$ and $|m\rangle$ to $(-|e\rangle + |m\rangle)/\sqrt{2}$. After the transformation, we have

$$\begin{aligned} U \otimes U|\Phi_{AB}^{+}\rangle &= |\Phi_{AB}^{+}\rangle, \\ U \otimes U|\Phi_{AB}^{-}\rangle &= |\Psi_{AB}^{+}\rangle, \\ U \otimes U|\Psi_{AB}^{+}\rangle &= -|\Phi_{AB}^{-}\rangle, \\ U \otimes U|\Psi_{AB}^{-}\rangle &= |\Psi_{AB}^{-}\rangle. \end{aligned} \tag{10}$$

Obviously, two states $|\Phi_{AB}^{+}\rangle$ and $|\Psi_{AB}^{-}\rangle$ remain themselves after the transformation, while $|\Phi_{AB}^{-}\rangle$ and $|\Psi_{AB}^{+}\rangle$ exchange. Once again, we inject two photons with the state $|L^{\downarrow}\rangle$ into the two subsystems. If the system is initially in the state $|\Phi_{AB}^{+}\rangle$, both the same detectors will respond when the photons are injected into the system after the transformation. On the contrary, for an initial state $|\Phi_{AB}^{-}\rangle$, two different detectors will respond. For the situation with $|\Psi_{AB}^{\pm}\rangle$, we will expect the same detectors to respond for $|\Psi_{AB}^{+}\rangle$ in contrast to two different detectors to respond for $|\Psi_{AB}^{-}\rangle$. Therefore, after the above two steps, the four Bell states are distinguished.

4. Conclusion

In the composite system consisting of four quantum dots and optical microcavities, we simulate the anyon states and the braiding operation is dynamically monitored by the braiding detecting gate (BDG). It is demonstrated that the BDG does not only work in our realization of the braiding operation but also acts in the scheme of Ref. [59]. Besides, we also show that the types of anyons and the four Bell states of anyons can be efficiently identified by the above BDG.

Although in the previous sections, we mainly propose to detect the anyon's braiding operation in the composite system of microcavities and quantum dots, we remark that circuit QED also provides us with a potential candidate for realizing our proposal. In Ref. [60], a two-level atom is also utilized to switch a single photon to coherently transport in the one-dimensional waveguide, which has recently been experimentally realized [61,62]. The reflection or transmission of the single photon may detect the atomic state without disturbing it.

Acknowledgments

This work was supported by the National Natural Science Foundation of China Grant No.11175094, the National Basic Research Program of China (2009CB929402, 2011CB9216002), and the Specialized Research Fund for the Doctoral Program of Education Ministry of China (20110002110007). QA thanks the National Science Council, Taiwan (Grant No. NSC 101-2811-M-002-148) for financial support.

References

[1] F. Wilczek, Phys. Rev. Lett. 48 (1982) 1144.
[2] J.M. Leinaas, J. Myrheim, Nuovo Cimento B 37 (1997) 1.
[3] F. Wilczek, Phys. Rev. Lett. 49 (1982) 957.
[4] F. Wilczek, Phys. Rev. Lett. 48 (1982) 1146.
[5] F. Wilczek, Phys. World 19 (2006) 22.
[6] Y. Shen, B.-Y. Jin, J. Phys. Chem. A 117 (2013) 12540.
[7] W.S. Dai, M. Xie, Ann. Phys. 332 (2013) 166.
[8] W.S. Dai, M. Xie, J. Stat. Mech. (2009) P04021.
[9] Y. Shen, Q. Ai, G.L. Long, Physica A 389 (2010) 1565.
[10] Y. Shen, C. Wang, G.L. Long, Physica A 390 (2011) 4713.
[11] Y. Shen, Q. Ai, G.L. Long, Comm. Theor. Phys. 56 (2011) 873.
[12] A.G. Truscott, K.E. Strecker, W.I. McAlexander, G.B. Partridge, R.G. Hulet, Science 291 (2001) 2570.
[13] A. Comtet, S.N. Majumdar, S. Ouvry, J. Phys. A 40 (2007) 11255.
[14] S. Mashkevich, S. Matveenko, S. Ouvry, Nuclear Phys. B 763 (2007) 431.
[15] A. Rovenchak, Low Temp. Phys. 35 (2009) 400.
[16] W.S. Dai, M. Xie, Physica A 331 (2004) 497.
[17] F. Schreck, L. Khaykovich, K.L. Corwin, G. Ferrari, T. Bourdel, J. Cubizolles, C. Salomon, Phys. Rev. Lett. 87 (2001) 080403.
[18] X.W. Guan, M.T. Batchelor, C. Lee, M. Bortz, Phys. Rev. B 76 (2007) 085120.
[19] Y. Shen, W.S. Dai, M. Xie, Phys. Rev. A 75 (2007) 042111.
[20] C.Y. Lu, W.B. Gao, O. Gühne, X.Q. Zhou, Z.B. Chen, J.W. Pan, Phys. Rev. Lett. 102 (2009) 030502.
[21] Y.J. Han, R. Raussendorf, L.M. Duan, Phys. Rev. Lett. 98 (2007) 150404.
[22] X.C. Yao, T.X. Wang, P. Xu, H. Lu, G.S. Pan, X.H. Bao, C.Z. Peng, C.Y. Lu, Y.A. Chen, J.W. Pan, Nature Photon. 6 (2012) 225.
[23] D. Boyanovsky, D. Jasnow, Physica A 177 (1991) 537.
[24] H.O. Frota, F.S. de Aguiar, Physica A 269 (1999) 418.
[25] A. Lavagno, P. Narayana Swamy, Physica A 389 (2010) 993.
[26] M.R. Ubriaco, Physica A 392 (2013) 4868.
[27] G.R. Feng, G.L. Long, R. Laflamme, Phys. Rev. A 88 (2013) 022305.
[28] A.Y. Kitaev, Ann. Phys. 321 (2006) 2.
[29] A.Y. Kitaev, Ann. Phys. 303 (2003) 2.
[30] A. Auffès-Garnier, C. Simon, J.M. Géard, J.P. Poizat, Phys. Rev. A 75 (2007) 053823.
[31] D.P. Divincenzo, Science 270 (1995) 255.
[32] C.H. Bennett, D.P. Divincenzo, Nature 404 (2000) 247.
[33] A. Ekert, R. Jozsa, Rev. Modern Phys. 68 (1996) 733.
[34] R. Raussendorf, H.J. Briegel, Phys. Rev. Lett. 86 (2001) 5188.
[35] M.A. Nielsen, I.L. Chuang, Quantum Computation and Quantum Information, Cambridge University Press, Cambridge, UK, 2000.
[36] C.H. Bennett, S.J. Wiesner, Phys. Rev. Lett. 69 (1992) 2881.
[37] X.S. Liu, G.L. Long, D.M. Tong, F. Li, Phys. Rev. A 65 (2002) 022304.
[38] F.G. Deng, X.H. Li, C.Y. Li, P. Zhou, H.Y. Zhou, Phys. Rev. A 72 (2005) 044301.
[39] F.G. Deng, X.H. Li, C.Y. Li, P. Zhou, H.Y. Zhou, Eur. Phys. J. D 39 (2006) 459.
[40] X.H. Li, P. Zhou, C.Y. Li, H.Y. Zhou, F.G. Deng, J. Phys. B 39 (2006) 1957.
[41] A.K. Ekert, Phys. Rev. Lett. 67 (1991) 661.
[42] C.H. Bennett, G. Brassard, N.D. Mermin, Phys. Rev. Lett. 68 (1992) 557.
[43] N. Gisin, G. Ribordy, W. Tittel, H. Zbinden, Rev. Modern Phys. 74 (2002) 145.
[44] F.G. Deng, G.L. Long, Phys. Rev. A 68 (2003) 042315.
[45] G.L. Long, X.S. Liu, Phys. Rev. A 65 (2002) 032302.
[46] C.H. Bennett, G. Brassard, S. Popescu, B. Schumacher, J.A. Smolin, W.K. Wootters, Phys. Rev. Lett. 76 (1996) 722.
[47] D. Deutsch, A. Ekert, R. Jozsa, C. Macchiavello, S. Popescu, A. Sanpera, Phys. Rev. Lett. 77 (1996) 2818.
[48] J.W. Pan, C. Simon, Ĉ. Brukner, A. Zellinger, Nature 410 (2001) 1067.
[49] C. Simon, J.W. Pan, Phys. Rev. Lett. 89 (2002) 257901.
[50] J.W. Pan, S. Gasparoni, R. Ursin, G. Weihs, A. Zellinger, Nature 423 (2003) 417.
[51] Y.B. Sheng, F.G. Deng, H.Y. Zhou, Phys. Rev. A 77 (2008) 042308.
[52] L. Xiao, C. Wang, W. Zhang, Y.D. Huang, J.D. Peng, G.L. Long, Phys. Rev. A 77 (2008) 042315.
[53] C.H. Bennett, H.J. Bernstein, S. Popescu, B. Schumacher, Phys. Rev. A 53 (1996) 2406.
[54] B.S. Shi, Y.K. Jiang, G.C. Guo, Phys. Rev. A 62 (2000) 054301.
[55] T. Yamamoto, M. Koashi, N. Imoto, Phys. Rev. A 64 (2001) 012304.
[56] Z. Zhao, J.W. Pan, M.S. Zhan, Phys. Rev. A 64 (2001) 014301.
[57] Z. Zhao, T. Yang, Y.A. Chen, A.N. Zhang, J.W. Pan, Phys. Rev. Lett. 90 (2003) 207901.
[58] T. Yamamoto, M. Koashi, S.K. Özdemir, N. Imoto, Nature 421 (2003) 343.
[59] X.Q. Xi, M.L. Hu, Phys. Rev. A 82 (2010) 024303.
[60] L. Zhou, Z.R. Gong, Y.-x. Liu, C.P. Sun, F. Nori, Phys. Rev. Lett. 101 (2008) 100501.
[61] O. Astafiev, A.M. Zagoskin, A.A. Abdumalikov Jr., Y.A. Pashkin, T. Yamamoto, K. Inomata, Y. Nakamura, J.S. Tsai, Science 327 (2010) 840.
[62] J.Q. You, F. Nori, Nature 474 (2011) 589.